Experimental Eye Research 197 (2020) 108112

Contents lists available at ScienceDirect

Experimental Eye Research

journal homepage: www.elsevier.com/locate/yexer

Cell compaction is not required for the development of gradient refractive index profiles in the embryonic chick lens

Kehao Wang[a], Masato Hoshino[c], Kentaro Uesugi[c], Naoto Yagi[b], Robert D. Young[c], Bethany E. Frost[c], Justyn W. Regini[c], Andrew J. Quantock[c], Barbara K. Pierscionek[d,*]

[a] Beijing Advanced Innovation Center for Biomedical Engineering, School of Biological Science and Medical Engineering, Beihang University, Beijing, China
[b] Japan Synchrotron Radiation Research Institute (Spring-8), 1-1-1, Kouto, Sayo-cho, Sayo-gun, Hyogo, 679-5198, Japan
[c] Structural Biophysics Group, School of Optometry & Vision Sciences, Cardiff University, Cardiff, CF24 4HQ, Wales, UK
[d] School of Life Sciences and Education, Staffordshire University, College Road, University Quarter, Stoke-on-Trent, Staffordshire, ST4 2DE, UK

ARTICLE INFO

Keywords:
Gradient refractive index
Ocular embryogenesis
Chick eye
Lens fibre cells
Compaction
Ossicles

ABSTRACT

The development of the eye requires the co-ordinated integration of optical and neural elements to create a system with requisite optics for the given animal. The eye lens has a lamellar structure with gradually varying protein concentrations that increase towards the centre, creating a gradient refractive index or GRIN. This provides enhanced image quality compared to a homogeneous refractive index lens. The development of the GRIN during ocular embryogenesis has not been investigated previously. This study presents measurements using synchrotron X-ray Talbot interferometry and scanning electron microscopy of chick eyes from embryonic day 10: midway through embryonic development to E18: a few days before hatching. The lens GRIN profile is evident from the youngest age measured and increases in magnitude of refractive index at all points as the lens grows. The profile is parabolic along the optic axis and has two distinct regions in the equatorial plane. We postulate that these may be fundamental for the independent central and peripheral processes that contribute to the optimisation of image quality and the development of an eye that is emmetropic. The spatial distributions of the distinct GRIN profile regions match with previous measurements on different fibre cell groups in chick lenses of similar developmental stages. Results suggest that tissue compaction may not be necessary for development of the GRIN in the chick eye lens.

1. Introduction

The optical system in the avian eye varies widely depending on the habitat of the bird and their visual requirements. The eye lens in all species, thus far measured, has a gradient of refractive index (GRIN) formed by the gradually changing concentrations of protein in successive cell layers (Pierscionek and Regini, 2012). The lens is responsible for accommodation in most species in which this process occurs. In the chick eye, the cornea is also thought to have some involvement in accommodation (Glasser and Howland, 1996). Investigations on the development of the cornea and lens have generally been conducted separately (Bassnett and Šikić, 2017; Coulombre and Coulombre, 1964; Kujawa-Hadryś et al., 2010; Meyer and O'Rahilly, 1959). The cornea in the chick eye connects with posterior segment of the eye through a relatively flat ciliary region that contains a ring of scleral ossicles, cartilage-like structures, that are thought to support the shape of the eye (Bayón et al., 2007). The distance between the lens and the retina, onto which image-carrying light rays are focussed, is relatively short. This requires high refractive power for good image quality. How the GRIN lens in the chick eye develops and how this is synchronised with the growth of the cornea and anterior segment have not been studied.

The chick lens has three distinct zones: a central spherical region with concentric shells of fibre cells that have formed sutures, a peripheral region consisting of elongating fibres that are attached to the anterior and posterior lens capsule, and an annular pad covering the anterior surface and the equator of the lens (Beebe et al., 2001; Kuszak et al., 1984). Like other vertebrates, the chick lens contains fibre cells at various stages of differentiation with new cells continuously produced throughout life by the epithelium adjacent to the anterior capsule (Bassnett and Winzenburger, 2003). These newly formed cells elongate

* Corresponding author.
E-mail addresses: wangkehao1003@gmail.com (K. Wang), hoshino@spring8.or.jp (M. Hoshino), ueken@spring8.or.jp (K. Uesugi), yagi@spring8.or.jp (N. Yagi), YoungRD@cf.ac.uk (R.D. Young), FrostB2@cardiff.ac.uk (B.E. Frost), ReginiJW@cf.ac.uk (J.W. Regini), QuantockAJ@cf.ac.uk (A.J. Quantock), barbara.pierscionek@staffs.ac.uk (B.K. Pierscionek).

https://doi.org/10.1016/j.exer.2020.108112
Received 28 April 2020; Received in revised form 1 June 2020; Accepted 3 June 2020
Available online 16 June 2020

at the equatorial region, to form sutures in the polar regions, losing their organelles during maturation. Nuclei and organelle degradation generally commences at embryonic day 12 (E12) in the chick lens (Bassnett and McNulty, 2003) and creates a central organelle free region that grows at a similar rate to that of the lens equator (Bassnett and McNulty, 2003; Beebe et al., 2001).

The transparency of eye lenses is maintained by the precisely organised arrangement of the fibre cells. The cross-section of lens fibre cells has a flat hexagonal shape with two longer sides and four short sides. The two longer sides adhere to adjacent cells in the radial direction and the four short sides connect with adjacent cells in the circumferential direction (Bassnett et al., 2011). Lens fibre cells are tightly bound by adhesive proteins and gap junctions, which reduce the intercellular dimensions (Bassnett et al., 2011). Adhesions and connections are likely to play a role in effecting shear stresses between lens fibres that will arise in an accommodating lens. Types of cell-cell adhesion complexes change from the lens border toward the centre (Beebe et al., 2001) and cellular fusions appear in deeper lens regions (Kuszak et al., 1985, 1989) that may serve as a pathway for cytoplasmic movement between adjacent cells (Bassnett et al., 2011). It is not clear whether remodelling or compaction of inner layer lens fibre cells with continued accrual of cells on the lens surface or indeed a genetic mechanism which predetermines the concentration of cytoplasmic proteins in successive lens layers, creates the gradient of protein distribution and thereby the GRIN structure. Investigations on development of the optics in the growing chicken embryo are needed to provide insights into how the GRIN is formed. This study describes measurements of the developing anterior segment of the chick eye using X-ray interferometric analysis.

2. Materials and methods

2.1. Tissue samples

Fertilized White Leghorn chicken eggs obtained from a commercial hatchery (Henry Stewart, Louth, UK), were maintained at 37.8 °C and 58–60% humidity in an Octagon 100 incubator (Brinsea Products Ltd, Sandford, UK). Embryos were removed at E10, 12, 14, 16, and 18 days and handled in accordance with the ARVO Statement for Use of Animals for Ophthalmic and Vision Research and local ethical rules. Six samples were used for all ages except E16 for which there were five samples. Eyes were dissected free and transferred intact to primary fixative solution.

2.2. Scanning electron microscopy (SEM)

Eyes were fixed in 2.5% glutaraldehyde/2% paraformaldehyde in 0.1 M sodium cacodylate buffer, pH 7.2 at room temperature for 2–4 days on a rotator. After washing in buffer, anterior segments were isolated and transferred to 10% NaOH with one change of solution over a period of 2 days, followed by washing in distilled water for 2 days. This was conducted to achieve cell maceration and remove the epithelial cells overlying the extracellular corneo-scleral matrix, together with non-collagenous material and to expose the subjacent fibrillar tissue. The samples were post-fixed in aqueous 2% tannic acid for 6 h, followed by 1% osmium tetroxide for 2 h, with washes in distilled water between and subsequently. Samples were dehydrated through a graded series of ethanol to 100% and immersed in hexamethyldisilazane (HMDS) in 3 stages over 24 h, with the HMDS allowed to evaporate in a fume hood. The dried specimens were then mounted individually using carbon cement (Leit C, Agar Scientific, Stansted, UK) onto aluminium SEM stubs and coated with gold in a sputtercoater (S15OA, Edwards UK). Anterior segment surface morphology was imaged with a secondary electron detector in a scanning electron microscope (SEM) (XL20, Eindhoven, The Netherlands) at 15 kV.

2.3. Synchrotron based X-ray Talbot interferometry

Fixed eye samples were measured at the bending magnet beamline BL20B2 at SPring-8, Japan using X-ray Talbot interferometry (Hoshino et al., 2010, 2011; Momose, 2005; Momose et al., 2003). The X-ray beam was fine-tuned to 25 keV by a Si(111) double-crystal monochromator and passed through two transmission gratings. The pattern thicknesses for the nickel phase grating (G1) and the gold absorption grating (G2) were 4.35 μm and 110 μm respectively; the pitch and pattern size areas for both gratings were 4.8 μm and 50 × 50 mm^2 respectively. The X-ray beam passage through the sample and the two gratings produces Moiré fringe patterns that are detected by a scientific CMOS detector (ORCA Flash 4.0. Hamamatsu Photonics). During measurements, samples were fixed on a rotator to enable collection of 900 projection images per sample; the absorption grating G2 was shifted relative to G1 using a 5-step fringe-scan method with a Piezo stage for phase retrieval. The scans collected produce differential phase images that are integrated to yield the final phase images. From the phase shift value obtained from the tomographic reconstruction, protein concentration is determined against a calibration using standards of known density (Hoshino et al., 2010, 2011). The refractive index of the lens, which is linearly related to the protein concentration (Barer and Joseph, 1954), was calculated using a specific refractive increment of 0.18 ml/g which is applicable to proteins (Hoshino et al., 2010, 2011). The time of measurement for each lens was 50 min. MatLab (ver. 2018b, Natick, Massachusetts, USA) was employed for the post-processing of data and a custom developed code, that reconstructed three-dimensional data generated by X-ray interferometric measurements, was used to produce the contour images of chick lenses.

3. Results

Protein concentrations in the mid-sagittal plane of the anterior segment of the chick eye, including the cornea, anterior chamber and the lens, are shown in the first row of Fig. 1 for five representative chick eyes at E10, E12, E14, E16 and E18. The protein concentration along the optic axis of each eye is shown below each image. At all measured ages, the lens has a significantly higher maximum protein concentration than the cornea. In both the lens and the cornea, protein concentration increases with age but the rate of increase in the lens is much greater than that in the cornea. In samples aged E16 and E18, bright spots, indicating high protein concentration, are evident in the limbal region.

Refractive index distributions in the sagittal planes, shown as contour plots with increments of 0.05 in refractive index between each adjacent contour line (Fig. 2), reveal that lens size increases rapidly with age as the lens shape undergoes change. The central contours are elliptical at E10 and E12 (shown in Fig. 2a and b) and progressively become more circular (Fig. 2c, d and e). These contours do not adhere to the lens shape and this is particularly evident in cortical regions which do not show the contour regularity seen in the central nuclear region. The distinction between the cortical and nuclear regions is very clear in the GRIN profiles in the equatorial plane (Fig. 2f); there is a kink at the point where the refractive index decreases from the maximum at the lens centre, then plateaus before decreasing at a much greater rate in the periphery. The GRIN profiles in the sagittal plane are approximately parabolic (Fig. 2g). The overall profile shapes are similar for all ages with refractive index values increasing at every point and causing an increase in depth and breadth of the GRIN profile with age (Fig. 2 f and g). The maximum value of refractive index increases with developmental age, with the sharpest rise occurring between ages E16 and E18 (Fig. 2h).

The equatorial dimensions for both the whole lens and the lens nucleus (defined by the central region with relatively regular contours), increase steadily with developmental age (Fig. 3a). In the sagittal direction there is an initial increase in the growth of the lens and nucleus from E10 to E12, followed by a plateauing between E12 to E14 before a

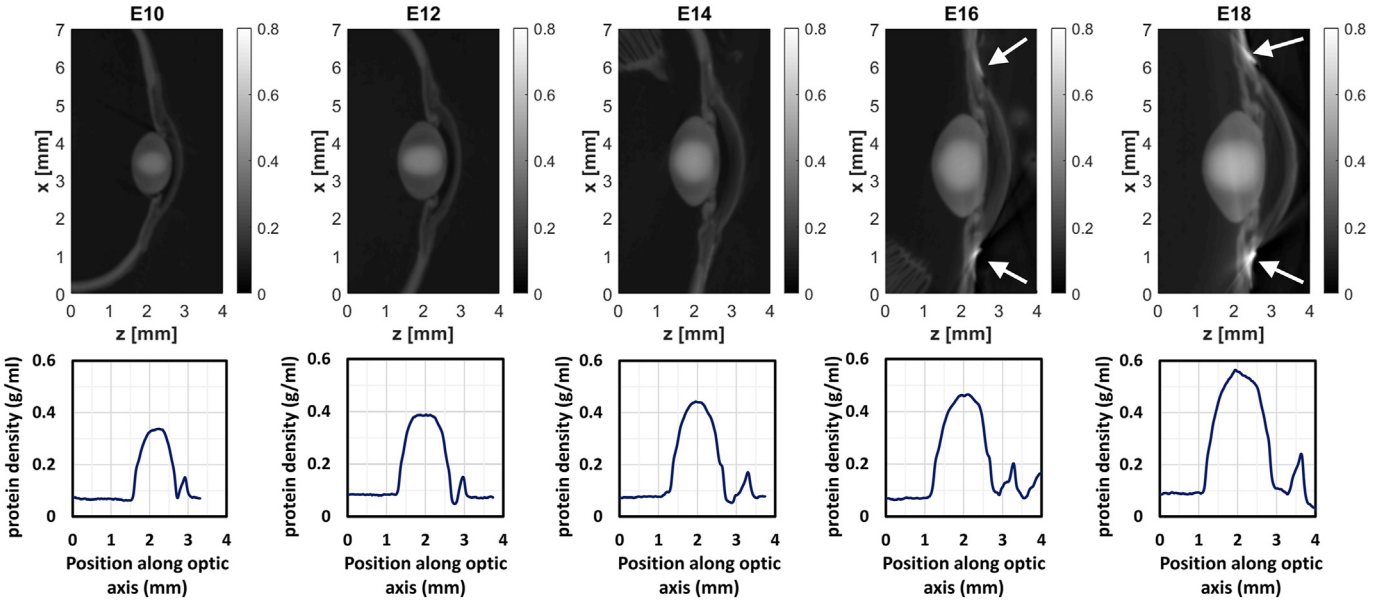

Fig. 1. Protein concentrations in mid-sagittal plane showing the anterior segment of five selected chick eyes at embryonic day (E) 10, 12, 14, 16, 18 (first row) and profiles of protein concentration along the optic axis of each chick eye (second row). Magnitude of protein concentration is indicated using the grey-scale intensity bar on the right side of each image (in g/ml). Peaks of very high density in the limbal regions of samples from ages E16 and E18 are indicated by arrows.

further increase from E14 to E18 (Fig. 3b). The lens becomes more elongated as it grows, manifesting in faster growth in the equatorial plane compared to the sagittal plane.

Fig. 4a shows GRIN profiles in the equatorial direction compared to the sizes of the central Organelle-Free Zone (OFZ) measured by Bassnett and McNulty (2003) for chick eyes at E13, E15 and E17 (taken from Fig. 6a in (Bassnett and McNulty, 2003)). The OFZ is similar in proportion to the plateau part of the GRIN in lenses of comparable age. Fig. 4b shows fibre cell positions based on results of a previous study (Faulkner-Jones et al., 2003) from a chick lens at age E19 with the GRIN profile in the equatorial plane for a lens aged E18. The size of the outermost region, containing fibre cells with both ends attached to lens capsule, correlates with the length of the plateau in the GRIN profile. The fibre cell regions where there is detachment from posterior and anterior capsules correspond to outer regions of the nuclear part of the GRIN profile, and the central RNA depletion region corresponds to the flatter, central portion of the GRIN profile (allowing for expansion of the E18 profile to age E19 and assuming there is no change in the overall shape).

SEM shows that the ossicles, a ring of fibrous bone connecting the cornea and sclera, are clearly visible beneath the ocular surface at E14 as fourteen discrete structures (Fig. 5a). At E16 these features become larger and start to connect with each other forming small protrusions between adjacent ossicles (Fig. 5b), and by E18 they have grown and merged further (Fig. 5c). Cross-sectional images of the protein density map show the same results (Fig. 5d–f). Brightness of the fourteen

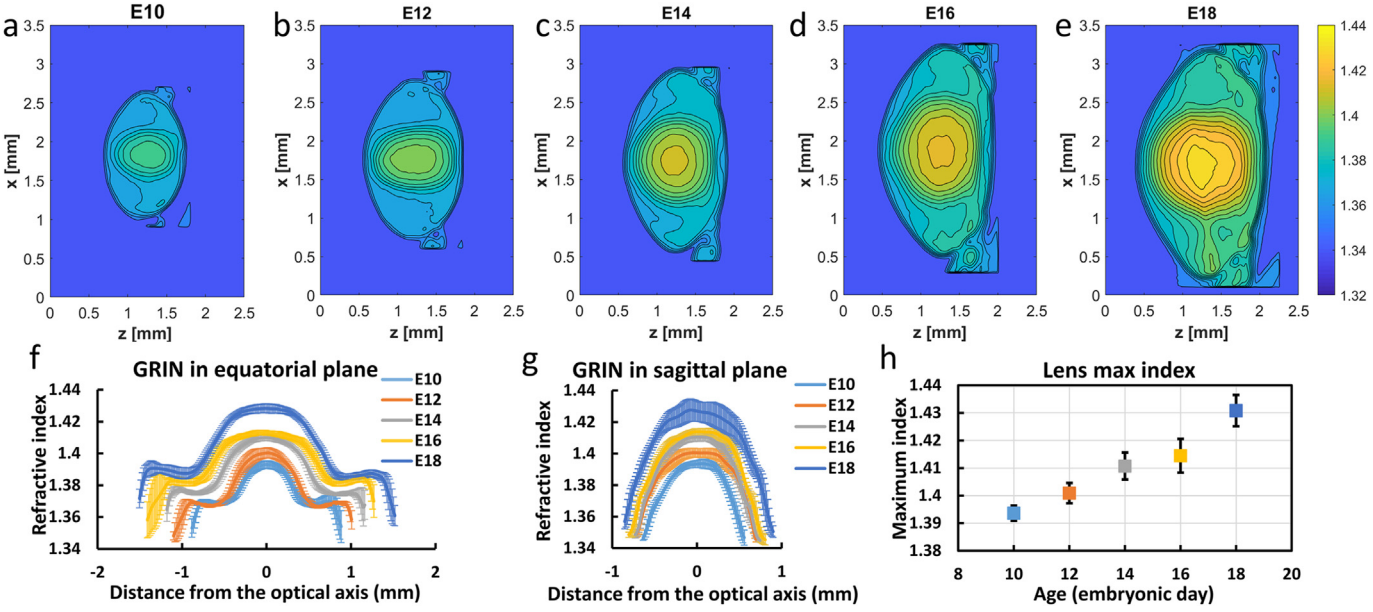

Fig. 2. Refractive index contours in chick lens at (a) E10, (b) E12, (c) E14, (d) E16 and (e) E18 (the interval of adjacent refractive index contours is 0.05), (f) refractive index profiles in the equatorial direction with error bars showing standard deviations and (g) along optic axis in the sagittal direction with error bars showing standard deviations at all five measured ages and (h) the maximum refractive index values plotted against age.

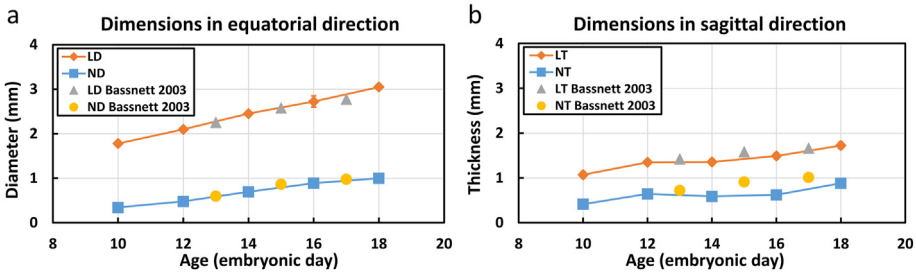

Fig. 3. Increase in lens dimensions with embryonic development for the whole lens and lens nucleus as well as comparison to results reported by Bassnett and McNulty (2003) in (a) equatorial direction and (b) sagittal direction.

ossicles increases from E14 (Fig. 5d) to E18 (Fig. 5f) indicating a density increase. Three-dimensional density profiles of the ossicles, with respect to the other anterior segment structures, are shown in Fig. 6.

4. Discussion

The presence of a GRIN profile in the eye lens is necessary for correcting aberrations and ensuring the highest possible image quality for the eye. The lens is not an isolated optical component but is an integral part of the eye in maturity and during formation; development of the lens can significantly influence development of other ocular tissues (reviewed in Bassnett and Šikić, 2017). For example, natural apoptotic cell death in the lens of a cave-dwelling form of *Astyanax mexicanus* has been shown to trigger atrophy of other ocular structures, with growth restored by transplantation of a lens from a surface-dwelling form (Yamamoto and Jeffery, 2000). Surgical removal of the lens from embryonic chick eyes has also been shown to prohibit the formation of the cornea and an anatomically normal anterior eye (Beebe and Coats, 2000; Young et al., 2019).

As new fibre cells are synthesised and added to the lens surface, existing fibre cells become part of the inner and central lens regions and their cellular protein concentrations increase. It has been suggested that compaction causes cellular water to be extracted from the cytosol of interior lens fibres causing the increase in protein concentration (Bassnett and Costello, 2017). The nature of the compacting force, if it indeed exists, is not known. Whilst evidence to support compaction in the nuclei of adult human lenses has been reported (Al-Ghoul et al., 2001; Costello et al., 2013; Freel et al., 2003; Taylor et al., 1996), this is not the case for all species. No evidence of compaction has been reported for nine species of piscine lenses (Kozł·owski and Kröger, 2019a, 2019b). In the adult human lens, the cross-sectional area of fibre cells decreases from the lens surface to the lens centre: 24 μm^2 for those located less than 100 μm from the lens surface to 7 μm^2 for those in the nucleus (Costello et al., 2013). In the chick lens, however, fibre cells at different depths do not show much variation in their cross-sections (Kuszak et al., 1980; Stirling and Wakely, 1987). Also absent from the chick lens is the surface 'wrinkling 'seen in inner layers of human lenses and which has been considered to be a manifestation of compaction (Al-Ghoul et al., 2001; Freel et al., 2003; Taylor et al., 1996). Compaction has been suggested as a possible causal factor for the increase in the nuclear refractive index in the developing murine lens although this was not conclusive (Cheng et al., 2019). However, a zone of compaction associated with cataract was found in the cortical region of ageing murine lenses (Cheng et al., 2019).

Compaction may be a causal factor in GRIN formation in some species but not in others. In the absence of compaction, the development of the GRIN profile is likely to be the result of a programmed protein and/or cell synthesis that ensures the requisite protein distribution for creating the GRIN. It is also possible that the nature of formation of the GRIN varies in different species, it is most likely to be multifactorial and depend not only on the growth mode, structural proteins and other mechanisms such as fluid microcirculation (reviewed in Donaldson et al., 2017) but on the functional properties, which are ultimately dictated by visual demand. Compaction also needs to be considered from the temporal aspect. A process of cell packing that occurs at a relatively rapid rate over a short period of time in developmental stages cannot be directly compared to one that takes years and may be influenced not just by growth but also by lens shape change in accommodation. Hence, it is not possible, without further investigation into the mechanism of compaction, to make comparisons between the results seen in adult human lenses (Al-Ghoul et al., 2001; Freel et al., 2003; Taylor et al., 1996) and those seen in animal lenses at early developmental stages.

The distributions and classes of crystallin proteins in the lens have been linked to the GRIN profile and refractive index magnitude (reviewed in Pierscionek and Regini, 2012). Notably lenses with high levels of γ-crystallin, such as found in rodents and fish, have steep GRIN profiles with high refractive index maxima and γ-crystallin is found in the greatest proportions in the nuclear region where refractive index is highest (reviewed in Pierscionek and Regini, 2012). This protein class has a propensity for tight packing (Slingsby, 1985; White et al., 1989; Srikanthan et al., 2004; Sagar et al., 2017) and a higher specific

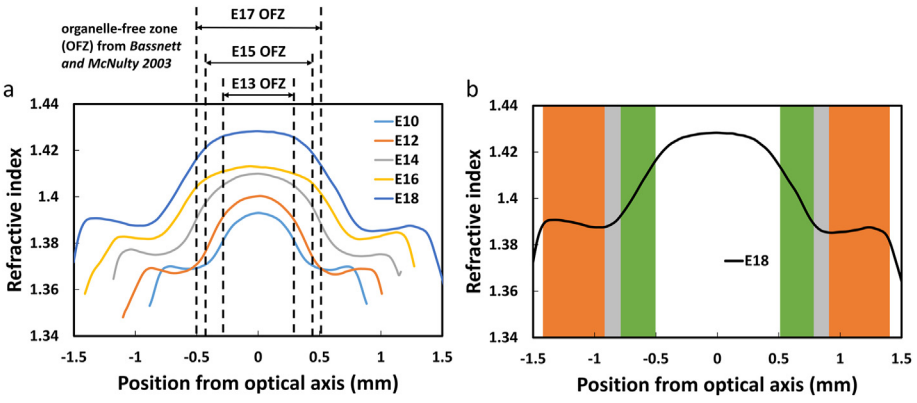

Fig. 4. Comparison of a) GRIN profiles of chick lenses at E10, E12, E14, E16 and E18 to sizes of central Organelle Free Zone (OFZ) of chick lenses aged E13, E15, E17 from Bassnett and McNulty (2003) and (b) GRIN profile from chick lens at E18 to locations of different lens fibres zones of a E19 chicken lens from Faulkner-Jones et al. (2003). Orange region: fibres attached to lens capsule; grey region: fibres detached from posterior lens capsule; green region: fibres detached from anterior lens capsule; white region: RNA depletion zone. (For interpretation of the references to colour in this figure legend, the reader is referred to the Web version of this article.)

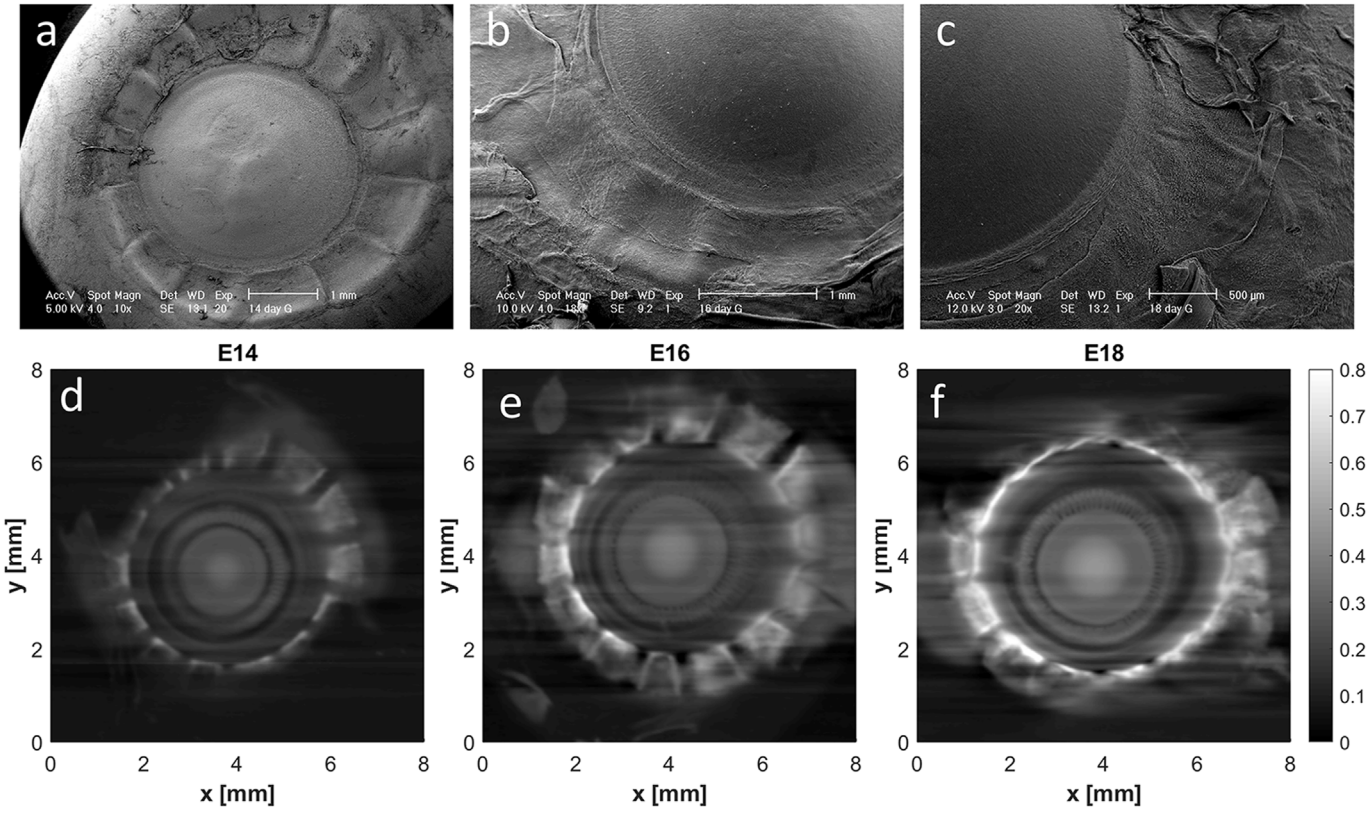

Fig. 5. Scanning electron microscopy images showing morphology of the anterior segment of the chick eye at (a) E14, (b) E16, (c) E18 and two-dimensional grey-scale images showing contours of protein density (in g/ml) and ossicles in the plane around 0.4 mm anterior to the equatorial plane, of chick eyes from ages (d) E14, (e) E16 and (f) E18.

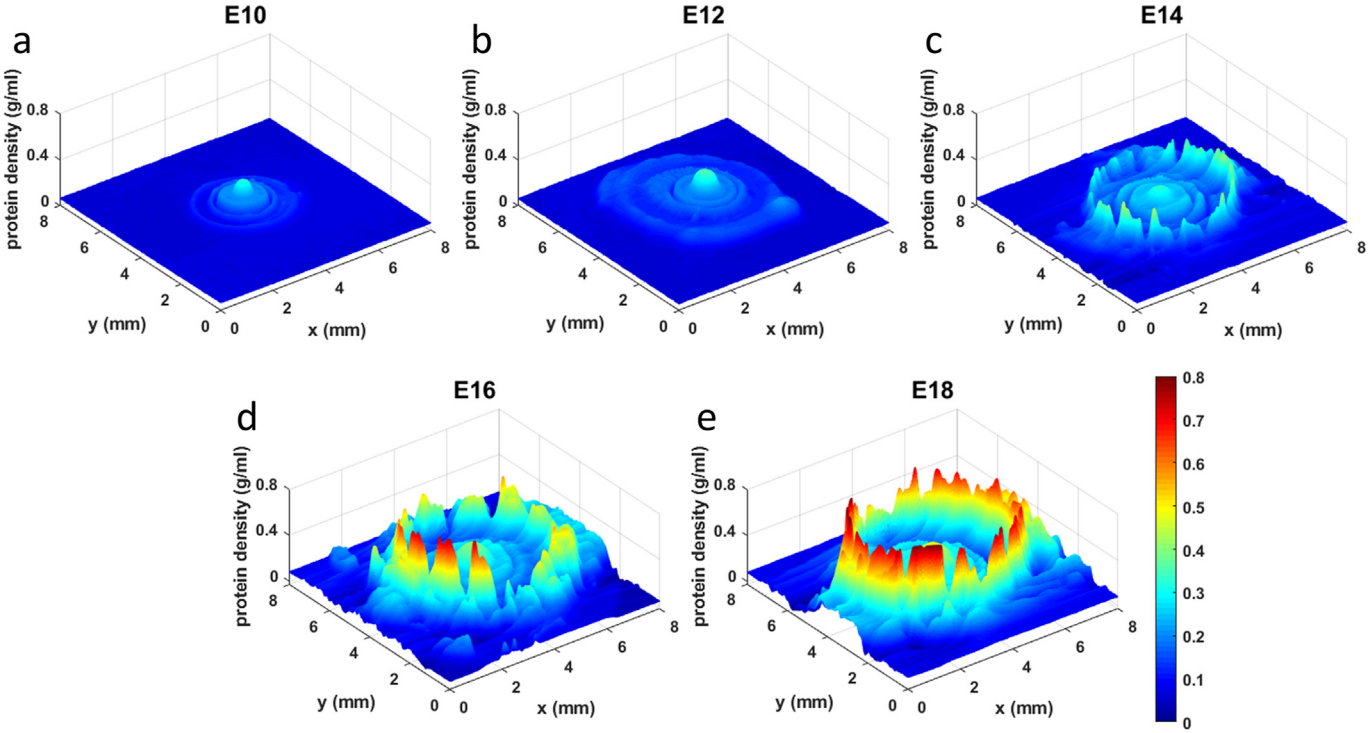

Fig. 6. Three-dimensional density profile (in g/ml) in the cross-sectional plane passing through the limbus of five selected chick eyes at (a) E10, (b) E12, (c) E14, (d) E16 and (e) E18 showing the emergence of the GRIN profile from E10 and the ossicles from E14.

refractive increment compared to the other crystallin classes (Pierscionek et al., 1987; Zhao et al, 2011a, 2011b; Khago et al., 2018). The chick lens contains very little γ-crystallin (Chen et al., 2016); its major protein is δ-crystallin, a protein that is soluble at very high concentrations, forms highly hydrated polymers and is found in softer, accommodating lenses (Simpson et al., 1995). The chick lens does not have a steep GRIN profile or high maximum refractive index and this is compatible with functional requirements, both optical and mechanical.

The specific refractive increment for δ-crystallin has not been reported. However, this protein is relatively abundant in amino acids, leucine and isoleucine (Piatigorsky et al., 1974; Piatigorsky, 1984) that have low molecular refractivity (Zhao et al., 2011a). The refractive increment of δ-crystallin will therefore be lower than those of the other crystallin classes (reviewed in Pierscionek and Regini, 2012). It should be noted that values of refractive increment of crystallin classes that have been measured (Pierscionek et al., 1987; Khago et al., 2018) and calculated (Zhao et al., 2011a, 2011b; Khago et al., 2018) vary widely. This is to be expected as refractive index depends on wavelength and to a lesser extent on temperature. In addition, proteins alter their conformation depending on their surroundings and interactions with other proteins; conformation (Khago et al., 2018) as well as amino acid sequence (Zhao et al., 2011a; Mahendiran et al., 2014; Khago et al., 2018) contribute to the value of the refractive increment. It cannot, therefore, be known precisely what the refractive increment will be at any given point *in situ* where there is a complement of different crystallins. Any possible variation in refractive increment from the value used in this study would only alter the refractive index magnitude in the third decimal place. The values given are not to this level of precision.

Our data show that the dimensions of the developing chick lens, and its nuclear region in the equatorial and sagittal planes, correspond well with published findings (Bassnett and McNulty, 2003). In particular, the centre of the GRIN profile (Fig. 4) closely matches with the size of OFZ zone (Bassnett and McNulty, 2003) where the cytosolic protein content reaches a maximum. In the central RNA depletion zone, the GRIN forms a plateau. It is feasible that cellular fusions in deeper lens regions allow for the free flow of cytosol between fibre cells (Kuszak et al., 1985, 1989), and hence contribute to maintaining a relatively uniform protein concentration in this region.

The refractive index contours in the developing chick lens do not follow the surface shape of the lens. This is not unexpected given the lenticular growth mode in which fibre cells, initially attached to both anterior and posterior capsule, progressively detach from the capsule while fibre cells in the equatorial region remain attached to the capsule (Faulkner-Jones et al., 2003). This produces the characteristic central region with isoindicial contours and an outer, equatorial section with less well-defined contours (Fig. 2a–e), resulting in the biphasic equatorial GRIN profile (Fig. 2f). This biphasic nature does not manifest in the GRIN profile along the optic axis (Fig. 2g). Here, the profile takes the parabolic form seen in many other species (Hoshino et al., 2011; Pierscionek and Regini, 2012) and is needed for unimpeded refraction and high image quality. A semblance of this refractive index distribution, in which the central region contours do not adhere to the surface shape of the lens, has been reported in equatorial GRIN profiles in young adult human lenses from the second (Pierscionek et al., 2015) and third decades (Pierscionek, 1997). In older human lenses the refractive index contours more closely follow the surface shape of the lens (Pierscionek et al., 2015). The young adult human lens, however, does not show the pronounced biphasic shape of the equatorial GRIN profile seen in the developing chick lens. The lack of data on the optics of the developing human lens prevents more detailed comparison. A study, using optical fibre sensing on gestational bovine lenses (Pierscionek et al., 2003), found that there was no GRIN profile until about mid-gestation at which time the parabolic form started to appear. In zebrafish, the perfectly regular and smooth parabolic GRIN profile is evident at 15 days post fertilisation (Wang et al., 2020); in murine lenses, the GRIN profile is visible at 2 weeks and starts to become more regular by 6 weeks of age (Cheng et al., 2019).

Unlike the spherical and high-density zebrafish and murine lenses, the chick lens is an elliptical and softer structure that renders it capable of some structural malleability required for accommodation. Results from measurements of lens shape change during natural accommodation showing the entire lens in the chick eye have not been reported. If accommodation in the chick eye is caused by squeezing of the lens via the forces of ciliary muscle (Choh et al., 2002), it is not clear how the structural organisation of fibre cells, with those in peripheral regions adherent to the capsule, would make this more mechanically effective than in a structure with concentric layers throughout.

Ossicles in the chicken eye, which start to develop at E14 are considered to allow the lens a greater range of movement (Choh et al., 2002) and the cornea to contribute to accommodation (Glasser et al., 1994; Schaeffel and Howland, 1987). The function of the ossicles is not fully understood. A study on the developing chick eye found asymmetries in ossicle number in just under half of the embryos examined (Franz-Odendaal, 2008). If ossicles are indeed critical to the accommodative process in the chick eye, this could suggest an asymmetry in accommodation between the two eyes. A functional reason for this is not clear and it is unlikely that such an asymmetry would be optically beneficial. The diversity in ossicle number and shape in the chick eye and in other species is reviewed in Fischer and Schoenemann (2019). How, and whether, the ossicles are involved in accommodation has not been determined (Fischer and Schoenemann, 2019). Further work on how the development of these structures are coordinated and exactly how the chick lens alters shape during naturally induced accommodation *in vivo* is needed to fully understand the contribution of all components of accommodation and the underlying opto-mechanical relationship in the lens.

Unlike primates, the chick retina does not have a fovea (Slijkerman et al., 2015) but an afoveate 'area centralis' of 3 mm diameter (Morris, 1982; Wisely et al., 2017). Variations in visual acuity in the centre and in the periphery of the 'area centralis' vary by only a factor of two (Ehrlich, 1981), which is far smaller than for foveae in human eyes (Seidemann et al., 2002). Emmetropisation in the periphery of the chick eye was found to have no influence on central refraction (Schipper and Schaeffel, 2006) unlike in the primate eye (Smith et al., 2005). This may have implications for the GRIN profile. In eyes where high visual acuity is concentrated in the fovea, the GRIN profile along the optic axis and paraxial region is of paramount importance. In eyes where the peripheral retina also has a reasonable degree of visual acuity, wider regions of the GRIN profile may contribute to providing the requisite image quality for emmetropisation.

Author contributions

B.E. Frost, R.D. Young and A.J. Quantock prepared the samples and SEM images. K. Wang, M. Hoshino, K. Uesugi, N. Yagi and B.K. Pierscionek conducted the beamtime measurements. K. Wang, M. Hoshino and B K Pierscionek performed the data analysis. K. Wang and B.K Pierscionek prepared the figures and the first draft of the manuscript. All other authors contributed to the final draft. K. Wang and B K Pierscionek conducted the revision.

Declaration of competing interest

None.

Acknowledgements

The authors acknowledge the funding support of beam time grants at SPring-8 synchrotron (grant no 2016A1096, 2017A1197, 2018A1105); Royal Society (grant no IE160996); Zeiss Meditec AG; Fight for Sight UK (1319/1320).

References

Al-Ghoul, K.J., Nordgren, R.K., Kuszak, A.J., Freel, C.D., Costello, M.J., Kuszak, J.R., 2001. Structural evidence of human nuclear fiber compaction as a function of ageing and cataractogenesis. Exp. Eye Res. 72, 199–214.

Barer, R., Joseph, S., 1954. Refractometry of living cells. Part 1. Basic Principles. Q. J. Microsc. Sci. 95, 399–423.

Bassnett, S., Costello, M.J., 2017. The cause and consequence of fiber cell compaction in the vertebrate lens. Exp. Eye Res. 156, 50–57.

Bassnett, S., McNulty, R., 2003. The effect of elevated intraocular oxygen on organelle degradation in the embryonic chicken lens. J. Exp. Biol. 206, 4353–4361.

Bassnett, S., Šikić, H., 2017. The lens growth process. Prog. Retin. Eye Res. 60, 181–200.

Bassnett, S., Winzenburger, P.A., 2003. Mophometric analysis of fibre cell growth in the developing chicken lens. Exp. Eye Res. 76, 291–302.

Bassnett, S., Shi, Y., Vrensen, G.F.J.M., 2011. Biological glass: structural determinants of eye lens transparency. Philos. Trans. R. Soc. Lond. B Biol. Sci. 366, 1250–1264.

Bayón, A., Almela, R.M., Talavera, J., 2007. Avian ophthalmology. Eur. J. Companion Anim. Pract. 17, 253–266.

Beebe, D.C., Coats, J.M., 2000. The lens organizes the anterior segment: specification of neural crest cell differentiation in the avian eye. Dev. Biol. 220, 424–431.

Beebe, D.C., Vasiliev, O., Guo, J., Shui, Y.B., Bassnett, S., 2001. Changes in adhesion complexes define stages in the differentiation of lens fiber cells. Invest. Ophthalmol. Vis. Sci. 42, 727–734.

Chen, Y., Sagar, V., Len, H.-S., Peterson, K., Fan, J., Mishra, S., McMurtry, J., Wilmarth, P.A., David, L., Wistow, G., 2016. γ-Crystallins of the chicken lens: remnants of an ancient vertebrate gene family in birds. FEBS J. 283, 1516–1530.

Cheng, C., Parreno, J., Nowak, R.B., Biswas, S.K., Wang, K., Hoshino, M., Uesugi, K., Yagi, N., Moncaster, J.A., Lo, W.K., Pierscionek, B., Fowler, V.M., 2019. Age-related changes in eye lens biomechanics, morphology, refractive index and transparency. Aging 11, 12497–12531.

Choh, V., Sivak, J.G., Meriney, S.D., 2002. A physiological model to measure effects of age on lenticular accommodation and spherical aberration in chickens. Invest. Ophthalmol. Vis. Sci. 43, 92–98.

Costello, M.J., Mohamed, A., Gilliland, K.O., Fowler, W.C., Johnsen, S., 2013. Ultrastructural analysis of the human lens fiber cell remodelling zone and the initiation of cellular compaction. Exp. Eye Res. 116, 411–418.

Coulombre, A.J., Coulombre, J.L., 1964. Lens development. I. Role of the lens in eye growth. J. Exp. Zool. 156, 39–47.

Donaldson, P.J., Grey, A.C., Heilman, B.M., Lim, J.C., Vaghefi, E., 2017. The physiological optics of the lens. Prog. Retin. Eye Res. 56, e1–e24.

Ehrlich, D., 1981. Regional specialization of the chick retina as revealed by the size and density of neurons in the ganglion cell layer. J. Comp. Neurol. 195, 643–657.

Faulkner-Jones, B., Zandy, A.J., Bassnett, S., 2003. RNA stability in terminally differentiating fibre cells of the ocular lens. Exp. Eye Res. 77, 463–476.

Fischer, O., Schoenemann, B., 2019. Why are bones in vertebrate eyes? Morphology, development and function of scleral ossicles in vertebrate eyes-a comparative study. J. Anat. Physiol. Stud. 3, 1–26.

Franz-Odendaal, T., 2008. Toward understanding the development of scleral ossicles in the chicken, *Gallus gallus*. Dev. Dynam. 237, 3240–3251.

Freel, C.D., Al-Ghoul, K.J., Kuszak, J.R., Costello, M.J., 2003. Analysis of nuclear fiber cell compaction in transparent and cataractous diabetic human lenses by scanning electron microscopy. BMC Ophthalmol. 3, 1.

Glasser, A., Howland, H.C., 1996. A history of studies of visual accommodation in birds. QRB (Q. Rev. Biol.) 71, 475–509.

Glasser, A., Troilo, D., Howland, H.C., 1994. The mechanism of corneal accommodation in chicks. Vis. Res. 34, 1549–1566.

Hoshino, M., Uesugi, K., Yagi, N., Mohri, S., 2010. Investigation of imaging properties of mouse eyes using X-ray phase contrast tomography. AIP Conf. Proc. 1266, 57–61.

Hoshino, M., Uesugi, K., Yagi, N., Mohri, S., Regini, J., Pierscionek, B., 2011. Optical properties of in situ eye lenses measured with X-ray Talbot interferometry: a novel measure of growth processes. PloS One 6, e25140.

Khago, D., Bierma, J.C., Roskamp, K.W., Kozlyuk, N., Martin, R.W., 2018. Protein refractive index increment is determined by conformation as well as composition. J. Phys. Condens. Matter 31, 435101.

Kozł-owski, T.M., Kröger, R.H., 2019a. Constant lens fiber cell thickness in fish suggests crystallin transport to denucleated cells. Vis. Res. 162, 29–34.

Kozł-owski, T.M., Kröger, R.H., 2019b. Visualisation of adult fish lens fiber cells. Exp. Eye Res. 181, 1–4.

Kujawa-Hadryś, M., Tosik, D., Bartel, H., 2010. Changes in thickness of each layer of developing chicken cornea after administration of caffeine. Folia Histochem. Cytobiol. 48, 273–277.

Kuszak, J., Alcala, J., Maisel, H., 1980. The surface morphology of embryonic and adult chick lens-fiber cells. Am. J. Anat. 159, 395–410.

Kuszak, J.R., Bertram, B.A., Macsai, M.S., Rae, J.L., 1984. Sutures of the crystalline lens: a review. Scanning Electron. Microsc. 1369–1378.

Kuszak, J.R., Macsai, M.S., Bloom, K., Rae, J., Weinstein, R., 1985. Cell-to-cell fusion of lens fiber cells in situ: correlative light, scanning electron microscopic, and freeze-fracture studies. J. Ultrastruct. Res. 93, 144–160.

Kuszak, J.R., Ennesser, C.A., Bertram, B.A., Imherr-McMannis, S., Jones-Rufer, L.S., Weinstein, R.S., 1989. The contribution of cell-to-cell fusion to the ordered structure of the crystalline lens. Lens Eye Toxic. Res. 6, 639–673.

Mahendiran, K., Elie, C., Nebel, J.-C., Ryan, A., Pierscionek, B.K., 2014. Primary sequence contribution to the optical function of the eye lens. Sci. Rep. 4, 5195.

Meyer, D.B., O'Rahilly, R., 1959. The development of the cornea in the chick. J. Embryol. Exp. Morphol. 7, 303–315.

Momose, A., 2005. Recent advances in X-ray phase imaging. Jpn. J. Appl. Phys. 44 (Part1), 6355–6367.

Momose, A., Kawamoto, S., Koyama, I., Hamaishi, Y., Takai, K., Suzuki, Y., 2003. Demonstration of X-ray Talbot interferometry. Jpn. J. Appl. Phys. 42 (Part2), L866–L868.

Morris, V.B., 1982. An afoveate area centralis in the chick retina. J. Comp. Neurol. 210, 198–203.

Piatigorsky, J., 1984. Delta crystallins and their nucleic acids. Mol. Cell. Biochem. 59, 33–56.

Piatigorsky, J., Zelenka, P., Simpson, R.T., 1974. Molecular weight and subunit structure of delta-crystallin from embryonic chick lens fibers. Exp. Eye Res. 18, 435–446.

Pierscionek, B.K., 1997. Refractive index contours in the human lens. Exp. Eye Res. 64, 887–893.

Pierscionek, B.K., Regini, J.W., 2012. The gradient index lens of the eye: an opto-biological synchrony. Prog. Retin. Eye Res. 31, 332–349.

Pierscionek, B., Smith, G., Augusteyn, R.C., 1987. The refractive increments of bovine α-,β- and γ-crystallins. Vis. Res. 27, 1539–1541.

Pierscionek, B.K., Belaidi, A., Bruun, H.H., 2003. Optical development in the foetal bovine lens. Exp. Eye Res. 77, 639–641.

Pierscionek, B., Bahrami, M., Hoshino, M., Uesugi, K., Regini, J., Yagi, N., 2015. The eye lens: age-related trends and individual variations in refractive index and shape parameters. Oncotarget 6, 30532–30544.

Sagar, V., Chaturvedi, S.K., Schuck, P., Wistow, G., 2017. Crystal structure of chicken γS-crystallin reveals lattice contacts with implications for function in the lens and the evolution of the βγ-crystallins. Structure 25, 1068–1078.

Schaeffel, F., Howland, H.C., 1987. Corneal accommodation in chick and pigeon. J. Comp. Physiol. A. 160, 375–384.

Schipper, R., Schaeffel, F., 2006. Peripheral defocus does not necessarily affect central refractive development. Vis. Res. 46, 3935–3940.

Seidemann, A., SchaeVel, F., Guirao, A., Lopez-Gil, N., Artal, P., 2002. Peripheral refractive errors in myopic, emmetropic, and hyperopicyoung subjects. J. Opt. Soc. Am. 19, 2363–2373.

Simpson, A., Moss, D., Slingsby, C., 1995. The avian eye lens protein δ-crystallin shows a novel packing arrangement of tetramers in a supramolecular helix. Structure 3, 403–412.

Slijkerman, R.W.N., Song, F., Astuti, G.D.N., Huynen, M.A., van Wijk, E., Stieger, K., Collin, R.W.J., 2015. The pros and cons of vertebrate animal models for functional and therapeutic research on inherited retinal dystrophies. Prog. Retin. Eye Res. 48, 137–159.

Slingsby, C., 1985. Structural variation in lens crystallins. Trends Biochem. Sci. 10, 281–284.

Smith III, E.L., Kee, C.S., Ramamirtham, R., Qiao-Grider, Y., Hung, L.F., 2005. Peripheral vision can influence eye growth and refractive development in infant monkeys. Invest. Ophthalmol. Vis. Sci. 46, 3965–3972.

Srikanthan, D., Bateman, O.A., Purkiss, A.G., Slingsby, C., 2004. Sulfur in human crystallins. Exp. Eye Res. 79, 823–831.

Stirling, R.J., Wakely, J., 1987. Changes in the surface morphology of lens fibres in the developing chick eye in relation to lens transparency. J. Anat. 155, 11–22.

Taylor, V.L., Al-Ghoul, K.J., Lane, C.W., Davis, V.A., Kuszak, J.R., Costello, M.J., 1996. Morphology of the normal human lens. Invest. Ophthalmol. Vis. Sci. 37, 1396–1410.

Wang, K., Vorontsova, I., Hoshino, M., Uesugi, K., Yagi, N., Hall, J.E., Schilling, T.F., Pierscionek, B.K., 2020. Optical Development in the Zebrafish Eye Lens. FASEBhttps://doi.org/10.1096/fj.201902607R.

White, H.E., Driessen, H.P., Slingsby, C., Moss, D.S., Lindley, P.F., 1989. Packing interactions in the eye-lens. Structural analysis, internal symmetry and lattice interactions of bovine gamma IVa-crystallin. J. Mol. Biol. 207, 217–235.

Wisely, C.E., Sayed, J.A., Tamez, H., Zelinka, C., Abdel-Rahman, M.H., Fischer, A.J., Cebulla, C.M., 2017. The chick eye in vision research: an excellent model for the study of ocular disease. Prog. Retin. Eye Res. 61, 72–97.

Yamamoto, Y., Jeffery, W.R., 2000. Central role for the lens in cave fish eye degeneration. Science 289, 631–633.

Young, R.D., Knupp, C., Koudouna, E., Ralphs, J.R., Ma, Y., Lwigale, P.Y., Jester, J.V., Quantock, A.J., 2019. Cell-independent matrix configuration in early corneal development. Exp. Eye Res. 187, 107772.

Zhao, H., Brown, P.H., Magone, M.T., Schuck, P., 2011a. The molecular refractive function of lens γ-crystallins. J. Mol. Biol. 411 (3), 680–699 Aug 19.

Zhao, H., Brown, P.H., Schuck, P., 2011b. On the distribution of protein refractive index increments. Biophys. J. 100, 2309–2317.